Opto-Electronic Science

Supplementary information

March 2023, Vol. 2, No. 3

DOI: 10.29026/oes.2023.220026

Multi-foci metalens for spectra and polarization ellipticity recognition and reconstruction

Hui Gao[1,2†*], Xuhao Fan[1†], Yuxi Wang[1†], Yuncheng Liu[1], Xinger Wang[1], Ke Xu[1], Leimin Deng[1,2], Cheng Zeng[1], Tingan Li[1], Jinsong Xia[1,2*] and Wei Xiong[1,2*]

[1]Wuhan National Laboratory for Optoelectronics and School of Optical and Electronic Information, Huazhong University of Science and Technology, Wuhan 430074, China; [2]Optics Valley Laboratory, Wuhan 430074, China.

[†]These authors contributed equally to this work.

*Correspondence: H Gao, E-mail: gaohui_wnlo@hust.edu.cn; JS Xia, E-mail: jsxia@hust.edu.cn; W Xiong, E-mail: weixiong@hust.edu.cn

This file includes:

Supplementary information for this paper is available at https://doi.org/10.29026/oes.2023.220026

Section 1: The physical mechanism of spectra and polarization ellipticity resolved multi-foci metalens (SPMM)

The SPMM consists of space-variant anisotropic sub-wavelength structures, which result in space-variant phase retardations by handedness-reversed circular cross-polarization conversion. Thus, the same construction of metalens performs as positive and negative lenses simultaneously for reversed handed-circular polarizations. The polarization-dependent metalens can be obtained by randomly mixing them, as shown in Fig. S1. The wavelength-dependent design is based on the holography principle.

We take the positive metalens for RCP design as an example. There are six discrete working wavelengths and six corresponding separated foci with different positions for this metalens. The positions of these six foci are expressed as

$$F(\lambda_n, \mathrm{R}) = (r, (n-1)\pi/3)\ , \tag{S1}$$

in the polar coordinate system as shown in the main body, which means the coordinate ($x_{\mathrm{center},n}$, $y_{\mathrm{center},n}$) of n^{th} focus in a rectangular coordinate system can be written as:

$$\begin{cases} x_{\mathrm{center},n} = r \cdot \cos((n-1)\pi/3) \\ y_{\mathrm{center},n} = r \cdot \sin((n-1)\pi/3) \end{cases}, \tag{S2}$$

where $r = 200$ μm. The phase maps of metalenses for different working wavelengths can be described as follows:

$$\varphi_n(x,y) = (\sqrt{(x-x_{\mathrm{center},n})^2 + (y-y_{\mathrm{center},n})^2 + f^2} - f) \cdot k_n\ , \tag{S3}$$

where focal distance f=1000 μm and wave vector of n^{th} wavelength k_n=2π/λ_n. The calculation for LCP design is similar to the expression above.

The propagation of a light beam with a cross-polarized state is controlled by the whole phase map of the SPMM, while the non-conversion light beam maintains the original propagation state, as shown in Fig. S1(a–d). The conversion efficiency is related to the wavelength of the incident beam and the geometrical parameters of the subwavelength structures. The non-conversion light beam can be filtered out by the quarter-wave plate and polarizer, as shown in Fig. S1. The same sub-wavelength structures generate the opposite phase for incident light beams with the opposite circular polarization state owing to the polarization-dependence of the geometric phase. Thus, a metalens with focal length f can be designed for any specific circular polarization and acquires a conjugate phase map of the lens under reverse-handedness circular polarized light incidence. As shown in Fig. S1(a, b), the positive metalens (with off-axis focus f) designed for left-handed circularly polarized (LCP) light performs as negative metalens when illuminated by a right-handed circularly polarized (RCP) light beam, and vice versa (Fig. S1(c, d)). Indeed, the intensity of the focus on the focal plane resulting from the positive metalens is much higher than the divergent beam of the negative lens. To realize a polarization-dependent metalens with switchable foci, two metalenses with different working polarization ellipticity and off-axis foci are integrated. An example of this mixing approach is shown in Fig. S1(e). The sub-wavelength structures of positive metalenses for LCP or RCP light with corresponding off-axis foci are arranged in a rectangular distribution which can be treated as an abstractive $M \times N$ "matrix". Using this abstractive "LCP metalens matrix," a random binary $M \times N$ matrix $\boldsymbol{A}$ is generated to calculate the Hadamard product. In $\boldsymbol{A}$, "0" and "1" are encountered with equal probability. Similarly, the result of the Hadamard product of the abstractive "RCP metalens matrix" and (1–$\boldsymbol{A}$) can also be acquired. The polarization-dependent metalens design can be obtained by adding these two Hadamard product results together. The focal position of this metalens can be switched by changing the polarization of the incident light beam. In this design, we applied a random rather than a periodic binary matrix to avoid the potential grating diffraction effect. It should be noted that this randomly mixed metalens performs as a positive and a negative lens concurrently depending on whether the illuminating light beam is LCP or RCP. While compared with the focus of the positive lens, the intensity of the divergent beam of the negative lens is too weak to observe at the focal plane and, therefore, can be ignored.

Section 2: The spatial distribution of foci and images of SPMM

The designed multi-foci metalens was based on the multispectral holographic principle (complex amplitude superposition method), which can be used in multispectral metasurface devices, such as metalens[S1] and meta-hologram[S2] designs. The main advantage of this method is that metasurface devices can be designed based on simple anisotropic

nanostructures, which generate the same geometrical phase for multi-wavelengths. The designed multispectral metasurface devices based on this method possessed multi-foci or multi-images even at a single wavelength, but only one focus or image was located on the target plane or region.

Here, we coded six off-axis metalenses with transversely dispersive information at different working wavelengths into one piece of the metasurface. And the foci positions of these six off-axis metalenses were located at different coordinates (r, β) on the same focal plane (z=1000 μm) in the cylindrical coordinate system, as shown in Fig. S2(a). And Fig. S2(b) presents the light fields of six r–z planes with different β and shows the transversely dispersive properties. The different colors represent different wavelengths (blue: 500 nm, green: 540 nm, yellow: 580 nm, orange: 620 nm, red: 660 nm, red-brown: 700 nm).

As discussed above, metalens designed by this method possessed multi foci even at a single wavelength. Sketch Fig. S2(c) shows the spatial distribution of these foci in three-dimensional space. However, only one of them is located at the designed focal plane, as shown in Fig. S2(d). Therefore, the metalens proposed in our manuscript can achieve a transversely dispersive focusing function at six wavelengths. Moreover, the foci positions on the same focal plane can be switched by changing working wavelengths, which is difficult to achieve for other multispectral design methods.

As the SPMM design is based on six specific discrete wavelengths (λ_1–λ_6), the six light spots at the focal plane are all defocused when the wavelength of the incident beam is different from any of the designed wavelengths. However, the extent by which each spot is defocused differs, and there is still one light spot that is focused much better than the other five. For example, the total light intensity at $F(\lambda_1)$ is much higher than the other positions at the focal plane when the wavelength of the incident beam is approximately λ_1. In this way, the broadband spectrum is divided into six bands, and the chromatic aberrations in each band are limited to a small range. Therefore, the designed metalens can also be used over a broad range to identify the spectral bands of the incident light beam (see Fig. 3(b) in the manuscript).

Besides, the metalens proposed in our manuscript can also achieve multispectral imaging function. Here we take two wavelengths (marked as red and blue in Fig. S3(a)) as an example to discuss the imaging process. As we explained above, this example metalens (marked as SPMM in Fig. S3(a) to be coincident with the manuscript) possesses two red foci and two blue foci in the space, and only one red focus and one blue focus are located at the designed focal plane. According to the equation $\frac{1}{l_1}+\frac{1}{l_2}=\frac{1}{f}$, the designed imaging plane can be obtained, in which there are two clear images, red image (left red arrow of solid line on imaging plane) and blue image (right blue arrow of solid line on imaging plane). Since there are two existing foci that are not located at the designed focal plane, so there are two clear images that are not located at the designed imaging plane (the left blue arrow of the solid line over the imaging plane and the right red arrow of the solid line below imaging plane). However, only two blur images (messy light fields) can be observed on the designed imaging plane (the left blue arrow of the dashed line on the imaging plane and the right red arrow of the dashed line on the imaging plane). And to be noted that there are obvious position shifts between clear images and blur images on the imaging plane, which provided a clear route to achieve the detection and reconstruction of spectra bands.

Figure S3(b) shows a typical imaging result of SPMM under six wavelengths (500 nm, 540 nm, 580 nm, 620 nm, 660 nm, and 700 nm, in a left-handed circularly polarized state) illuminating. The object distance and image distance are 70 mm and 1014.5 μm, while the focal length of SPMM is 1000 μm. Six clear images at different wavelengths can be observed at different positions of the imaging plane. And there are several blur images around each clear image, as shown in the enlarged illustration of Fig. S3(b). The obvious position shifts between these blur images and clear images provide a reference region for the detection and reconstruction of wavelengths (spectra bands).

Section 3: The definition of value η representing the polarization ellipticity

The polarization ellipticity (e.g., linear, elliptical, and circular) of light can be determined by angle χ (ranging from −π/4 to π/4) of the polarization ellipse, as shown in Fig. 4(b). As known that the arbitrary polarization ellipticity can be described as a point P on the Poincare sphere (Fig. 4(c)), while latitude 2χ denotes the degree by which elliptically polarized light deviates from linearly polarized light. Define η=tan(χ) ranging from −1 to 1 to express the polarization ellipticity (e.g., linear, elliptical, and circular) while a linear polarization state corresponds to η=0, and LCP or RCP states correspond to η=±1. Other values of η represent elliptical polarization, while negative and positive values correspond to

left-handed and right-handed states, respectively.

Section 4: The focusing efficiency of SPMM

Firstly, the proposed metalens performed as a positive and a negative lens concurrently. Therefore, half the energy of incident light could be focused. Secondly, six foci can be obtained in the space at a single wavelength while only one focus was located at the designed focal plane, as shown in Fig. S2. Therefore, only 1/6 energy was focused on the designed focal position. Thirdly, the conversion efficiencies of nanostructure at different working wavelengths vary, as shown in Fig. 2(d). So, we could calculate the focusing efficiencies were 5.64%, 5.62%, 5.03%, 3.14%, 2.57%, and 1.5% at wavelengths of 500 nm, 540 nm, 580 nm, 620 nm, 660 nm, and 700 nm, respectively.

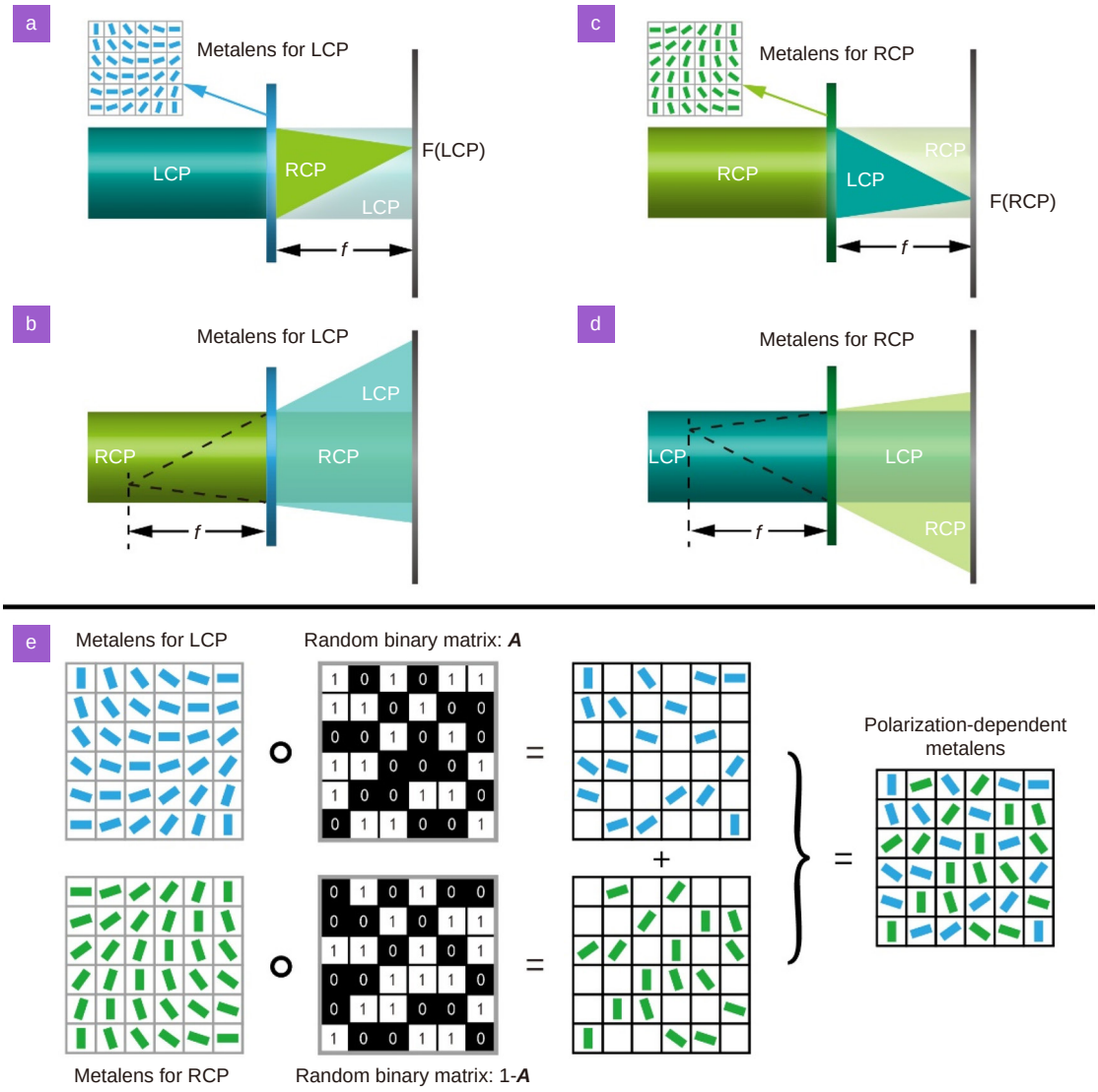

Fig. S1 | Design and physical mechanism of the polarization-dependent metalens. (**a**, **c**) The positive metalenses for LCP (or RCP) design convert an LCP (or RCP) light beam to RCP (or LCP) light and focus it at F(LCP) (or F(RCP)) on the focal plane. The conversion efficiencies are related to the wavelength of the incident beam and the geometrical parameters of the subwavelength structures. (**b**, **d**) The positive metalenses for LCP (or RCP) design perform as negative lenses when illuminated by an RCP (or LCP) light beam and generate divergent beams. (**e**) The metalenses for LCP (or RCP) design are treated as an abstractive $M \times N$ "matrix", and the Hadamard products of the LCP (or RCP) "matrix" and the random binary matrix $\boldsymbol{A}$ (or $(1-\boldsymbol{A})$) are calculated, respectively. The polarization-dependent metalens is acquired by adding these two Hadamard product results together.

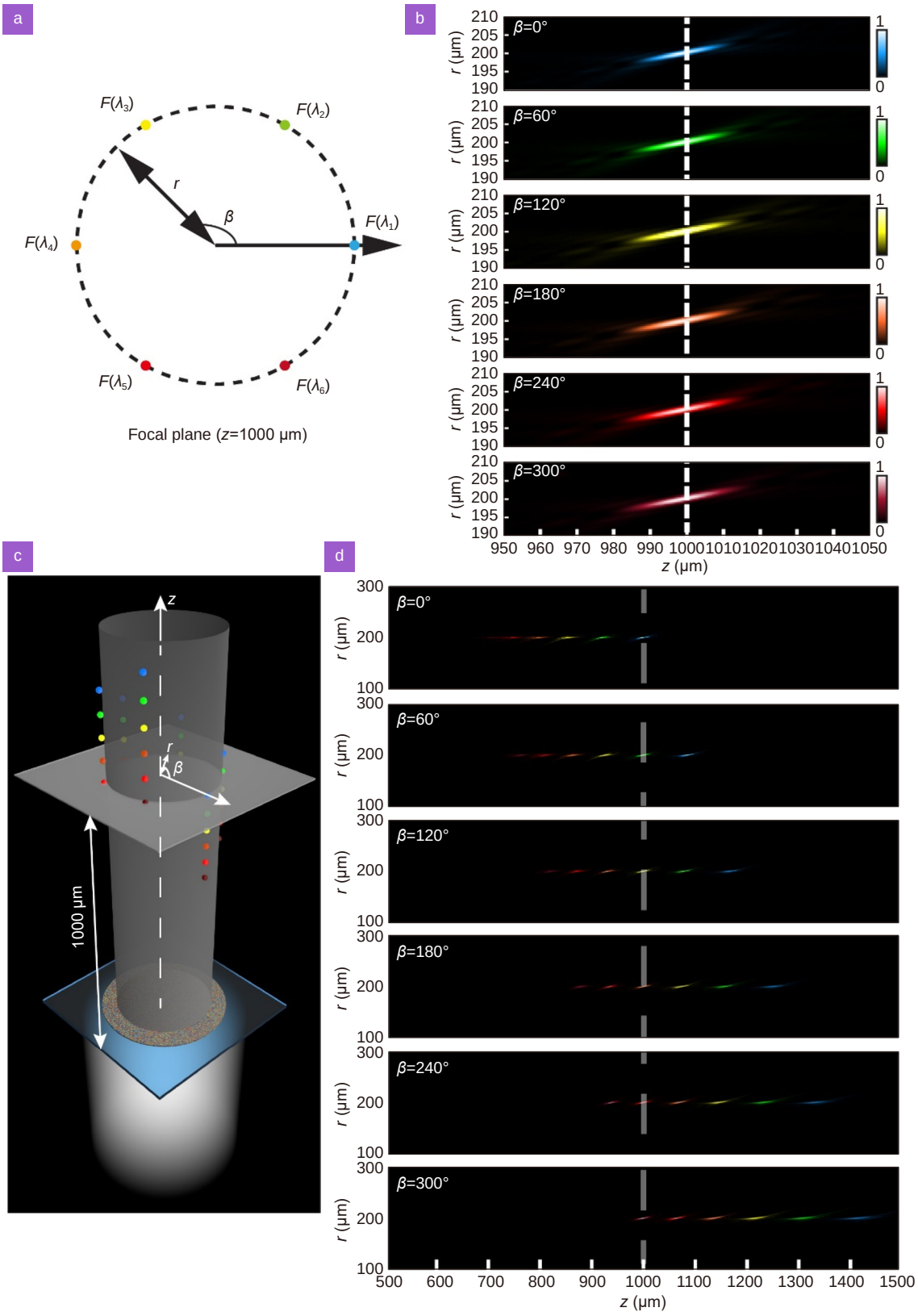

Fig. S2 | The transversely dispersive properties of designed metalens. (**a**) The sketch of foci positions at the focal plane. (**b**) The transversely dispersive focusing of six wavelengths. (**c**) The spatial distribution of 36 typical foci in three-dimensional space. (**d**) The light fields at the *r*-*z* plane with different *β*.

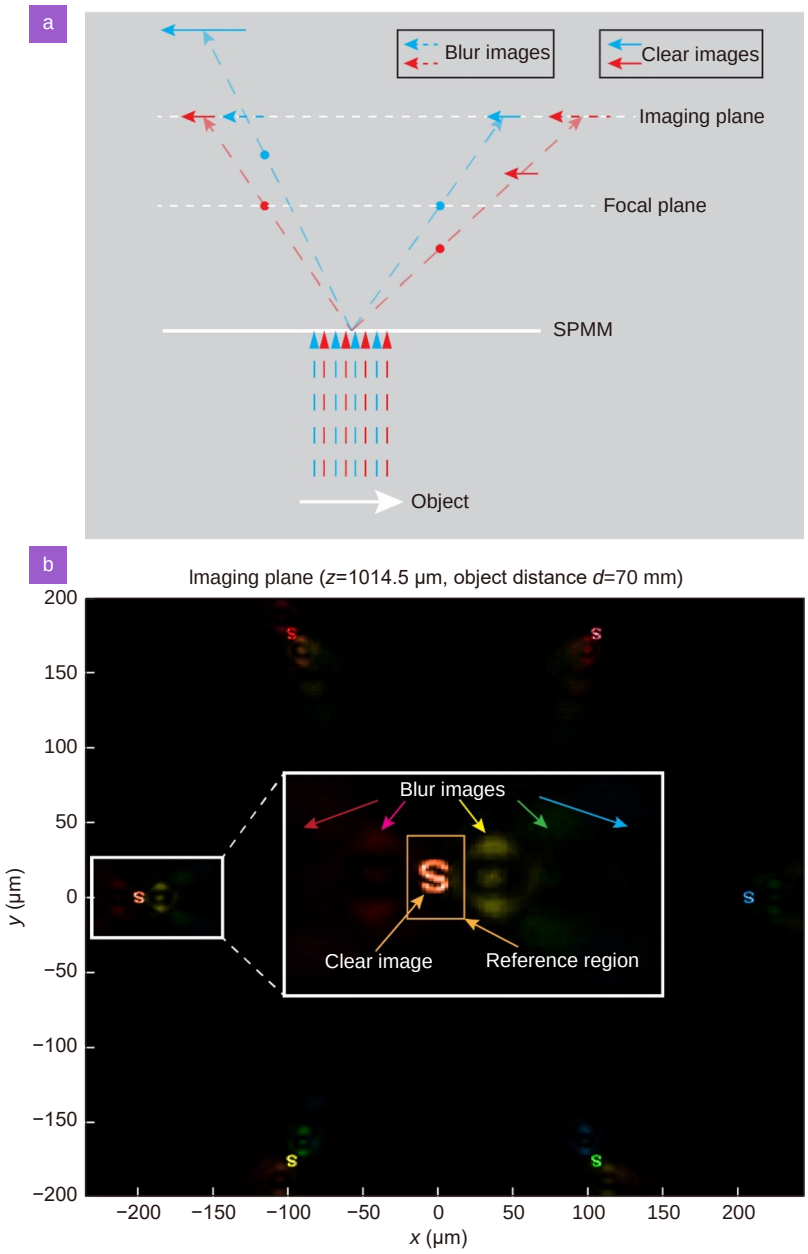

Fig. S3 | The sketch of the imaging process of SPMM. (**a**) Imaging process of SPMM with two working wavelengths. (**b**) The simulated imaging results of our proposed SPMM with the light illumination of six wavelengths.

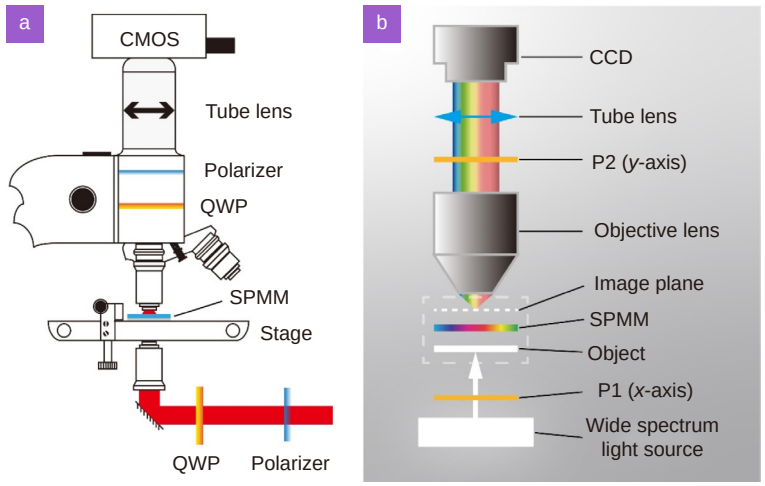

Fig. S4 | The experimental imaging system of SPMM with laser and ordinary light source. (**a**) The sketch map of the optical setup with a laser source. The elliptic polarization states of the incident laser beam are modulated by changing the rotation angle of a linear polarizer and a quarter-wave plate (QWP). The patterns of transmitted light are imaged by an objective lens and a tube lens, and are recorded by a CMOS camera (Daheng Imaging, MER-U3). The cross-conversion efficiencies of nanostructures are not 100%, which means that some non-conversion and non-modulation light beams are transmitted through the metasurface directly. A cascaded quarter-wave plate and a polarizer are used to filter the non-conversion background noise. (**b**) The sketch map of the optical setup with an ordinary light source. The object is illuminated by a wide spectrum light source, and twelve images are located at different positions on the imaging plane, which correspond to six different spectral bands and two kinds of polarizations. These twelve images are collected and recorded by a microscope system. P1 and P2 represent two polarizers with orthogonal directions, which are used in systems to reduce background noise.

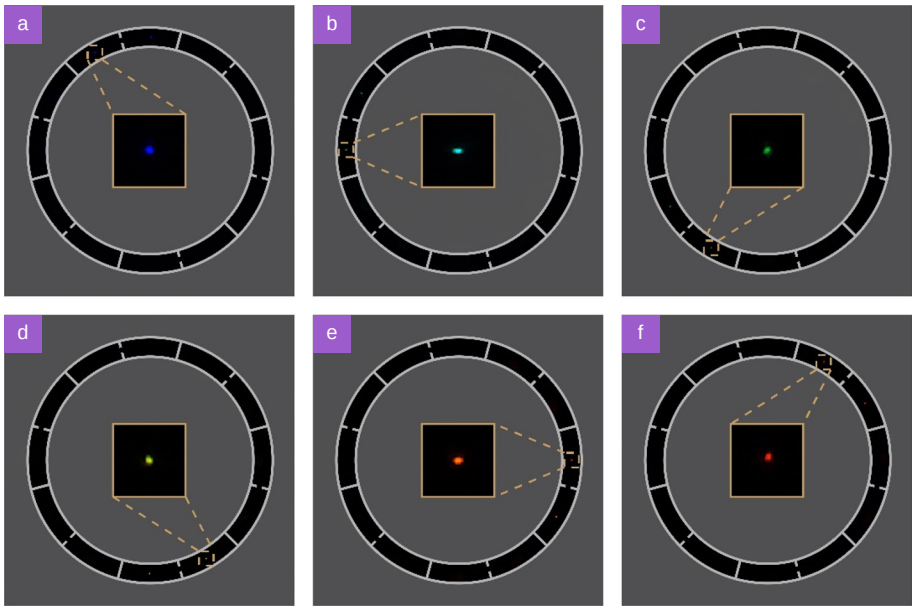

Fig. S5 | Focusing results of the SPMM for the incident light beam with six different sets of wavelengths.

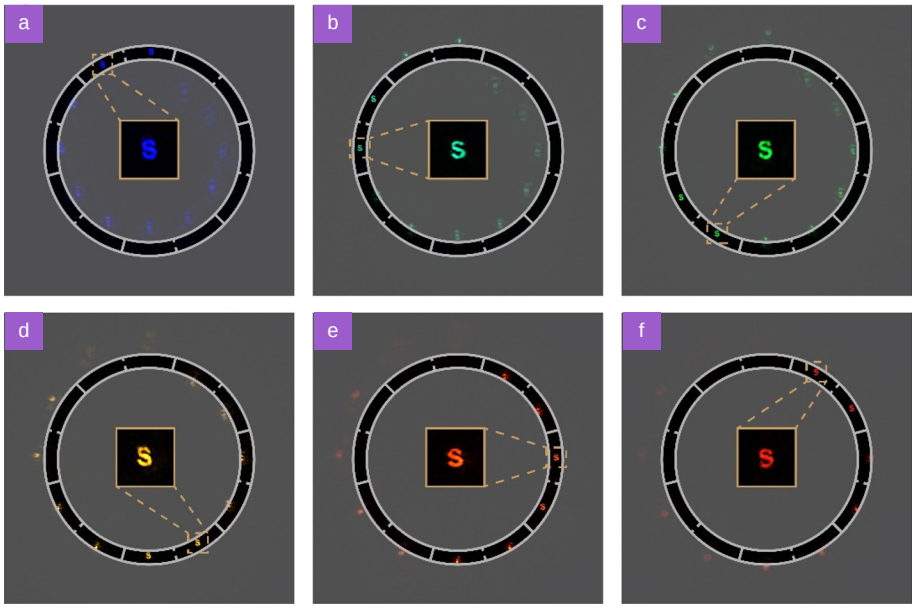

Fig. S6 | Imaging results for the pattern "S" with the incident light beam of six different sets of wavelengths.

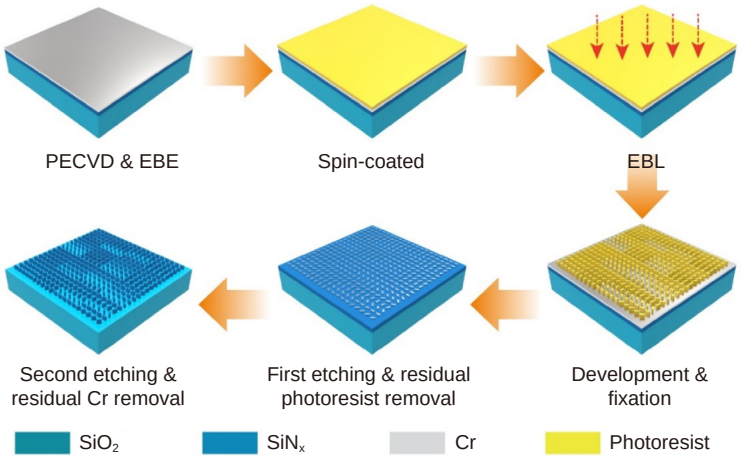

Fig. S7 | The fabrication of SPMM. The fabrication of the SPMM begins from a glass substrate with a thickness of 500 μm. A silicon nitride thin film of 600 nm thickness is coated by plasma-enhanced chemical vapor deposition onto the substrate. Next, a chromium film of thickness 20 nm is deposited by electron-beam evaporation on the SiN*x* layer as a hard mask. Then a 200 nm photoresist layer (CSAR62) is spin-coated onto the top of the Cr layer. The nanostructure patterns are written by electron-beam lithography (Vistec: EBPG 5000 Plus) and implemented into the photoresist layer after development. The pattern is then transferred into the Cr hard mask layer by inductively coupled plasma etching (ICP, Oxford Plasmalab: System100-ICP-180), and the residual photoresist is stripped off by an oxygen plasma stripper (Diener electronic: PICO plasma stripper). Finally, the pattern is transferred into the SiN*x* layer by the next ICP process, and the remaining Cr is removed by Cr corrosion solution. The Cr layer is utilized as a hard mask because of the extremely high etching selectivity between Cr and SiN*x*.

References

S1. Zhao ZY, Pu MB, Gao H, Jin JJ, Li X et al. Multispectral optical metasurfaces enabled by achromatic phase transition. *Sci Rep* **5**, 15781 (2015).

S2. Li X, Chen LW, Li Y, Zhang XH, Pu MB et al. Multicolor 3D meta-holography by broadband plasmonic modulation. *Sci Adv* **2**, e1601102 (2016).